Journal of Fish Biology (1998) **53,** 340–365
Article No. jb980703

Fine structure of the intestine development in cultured sea bream larvae

A. Calzada, A. Medina* and M. L. González de Canales

Departamento de Biología Animal, Biología Vegetal y Ecología, Facultad de Ciencias del Mar, Apartado 40, E-11510 Puerto Real, Cádiz, Spain

(*Received 4 November 1997, Accepted 31 March 1998*)

At hatching, the gut cells of *Sparus aurata* are quite undifferentiated; however, slight ultrastructural differences can already be distinguished between the presumptive intestinal regions. The hindgut cells are more differentiated than midgut cells and the rectal cells show rather particular ultrastructural features. During days 1 (D1) and 2 (D2) after hatching, major changes occur that lead to full differentiation of the epithelial cells. Shortly before the onset of exogenous feeding (D3), the anterior intestine enterocytes can synthesize lipoprotein particles (LP) from endogenous lipids. The posterior intestine enterocytes show morphological features indicating a role in absorption and intracellular digestion of nutrients, whereas the rectal cells do not. Transient ciliated cells occur at hatching (D0) in the presumptive intestine, except in the caudal rectum, and disappear at the start of the late endotrophic phase about 3 days after hatching (D3). At hatching, very scarce enteroendocrine and leucocyte-like cells are found at the base of the gut epithelium. Their number increases throughout development. At D3 (late endotrophic phase), LP synthesized mainly in the periblast invade the circulatory system, interstitial spaces of the subepithelial tissue and intercellular spaces of the gut epithelium. When the endo–exotrophic phase begins (D4), the enterocytes can absorb exogenous food. Acid phosphatase activity was detected in microvilli, apical vacuoles and Golgi complex in both anterior and posterior enterocytes, as well as in supranuclear vacuoles (SNV) of posterior enterocytes, but not in the apical tubulovesicular system (TVS). During the exotrophic phase, large lipid droplets (LD) are found in anterior enterocytes, and the SNV occupy a large cell volume in posterior enterocytes. LP accumulate first in extracellular spaces and then are transferred to the circulatory system. Mucous and rodlet cells appear in the intestinal epithelium during the exotrophic phase, from D15.

Key words: teleost; *Sparus aurata*; gut development; ultrastructure; lipid absorption; lipid droplets; lipoprotein particles; macromolecular absorption.

INTRODUCTION

From the time of hatching, teleost larvae must develop efficient structures and mechanisms for searching, capturing, absorbing and digesting food. As in other species (Blaxter, 1988), sea bream *Sparus aurata* L., larvae at the endotrophic phase possess limited endogenous energetic and nutritive reserves (Guyot *et al.*, 1993; Mani-Ponset *et al.*, 1996). Major morphological and functional changes must occur for the larva to survive one of the most critical stages of its life span, when these yolk reserves are almost exhausted. This is particularly important for marine species, where high rates of larval mortality during this period are recorded in culture (Fyhn, 1989). In this phase, sea bream larvae seem to have developed the mechanisms to absorb and digest exogenous food, since pancreatic

*Author to whom correspondence should be addressed.
Email: antonio.medina@uca.es

0022–1112/98/080340+26 $30.00/0

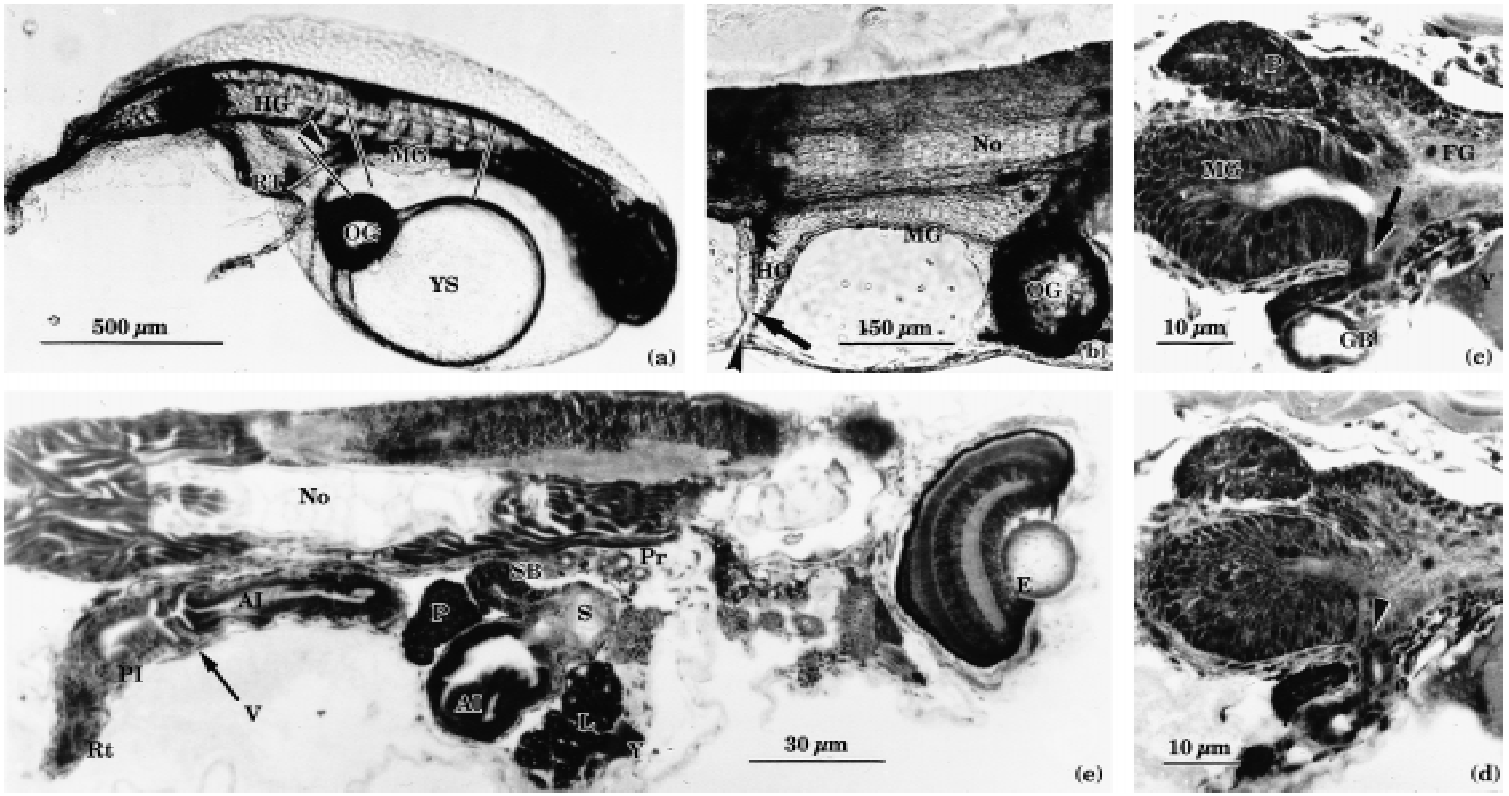

FIG. 1. Light microscopy, endotrophic phase. Whole larvae [(a) and (b)]. In (a) (D0), the midgut (MG) extends over the yolk sac (YS). In (b) (D1) the urinary bladder anlage merges with the gut (→) and the anus is open (►). Sagittal sections stained with toluidine blue [(c)–(e)]. (c) D2 larva showing the connection of the pancreatic duct with the gut (→). (d) A serial section close to that in (c) (distant ~7 μm). The biliary duct opens inside the gut, rostral to the pancreatic duct (►). (e) Overview of a D3 larva. AI, anterior intestine; E, eye; FG, foregut; GB, gall bladder; HG, hindgut; L, liver; MG, midgut; No, notochorda; OG, oil globule; P, pancreas; PI, posterior intestine; Pr, pronefros; Rt, rectal anlage; S, presumptive stomach; SB, swim bladder anlage; V, intestinal valve; Y, yolk.

and digestive enzymes have been detected, and the intestine shows a regional functional differentiation (Sarasquete *et al.*, 1993, 1995; Moyano *et al.*, 1996). Recent investigations have increased the success in the production of sea bream larvae (Mourente & Odriozola, 1990*a*,*b*; Polo *et al.*, 1992; Yúfera *et al.*, 1993*a*,*b*). Nowadays, an increasing tendency to replace live food with inert pellets (Fernández-Díaz *et al.*, 1994; Yúfera *et al.*, 1996) demands a good knowledge of the development of digestive and nutritional requirements of larvae during the stage when a functional stomach is not present and proteolytic gut capacities are still very limited (Moyano *et al.*, 1996). Therefore, morphological studies on the ontogeny of the digestive system, along with experimental investigation under changing feeding regimes will increase the knowledge of food requirements of larvae.

Although light microscope studies have provided wide information on the gut development in fishes, most of the available ultrastructural studies have paid particular attention to the cellular status just before the onset of exogenous feeding. In contrast, only a few reports (e.g. Connes & Benhalima, 1983; Kjørsvik & Reiersen, 1992; Otake *et al.*, 1995) have described the fine structure of gut cells at the early endotrophic phase. An overall histological view of *S. aurata* gut development has been provided by Sarasquete *et al.* (1993, 1995) and the effect of starvation on the feeding ability in this species was studied by Yúfera *et al.* (1993*b*). This paper studies the ultrastructural modifications occurring during the transition from the undifferentiated gut to a functional digestive tract in cultured *S. aurata* from hatching (day 0) to day 25 after hatching (D25). The aim is to contribute to knowledge of the functional status of the larval fish gut, to further understanding of larval fish biology and its management in culture, and to help in further nutritional studies.

MATERIALS AND METHODS

LARVAL SAMPLES

Sparus aurata larvae were reared from D0 to D25 in a commercial fish farm (CUPIMAR, S.A., San Fernando, Cádiz, Spain) at a density of 2000 larvae l^{-1} (D0–D2), 160 larvae l^{-1} (D3–D9), 90–120 larvae l^{-1} (D10–D19) and 40 larvae l^{-1} (D20–D25). The rearing temperature varied between 19°–20° C. The highest mortality was registered between D9 and D10. The turnover of water (pH 7·8, 32‰ salinity, 90% oxygen saturation) was maintained at 80%. A constant photoperiod (300 lx) was maintained.

Rotifers *Brachionus plicatilis* enriched with the microalga *Nannochloropsis gaditana* were supplied from D3 twice a day at a concentration of 6–10 rotifers ml^{-1}. From D15, *Artemia* sp. nauplii, enriched with Selco®, were added to maintain about 3 nauplii ml^{-1}. From D20, *Artemia* sp. metanauplii were introduced into the diet. Three different phases were distinguished during the larval development of sea bream: endotrophic phase from D0 to D4; endo-exotrophic phase from D4 to D10; and exotrophic phase from D10 to D25.

FIG. 2. Light microscopy, exotrophic phase. Sagittal sections of D25 larvae stained with toluidine blue [(a) and (b)]. (a) The anterior (AI) and posterior (PI) intestines are separated by the valvula (V). (b) The height of the brush border in proximal rectal cells decreases towards the anus (→). (c) Cross-section of D20 anterior intestine, Black Sudan stain. Lipid droplets (LD) predominate in the infranuclear cytoplasm. Sudanophilic inclusions (►) are also found in the apical cytoplasm, in the perinuclear region and in the intercellular spaces (IS). BB, Brush border; CT, connective tissue; F, food; L, lumen; N, nucleus; PI, posterior intestine; Rt, rectum; SV, supranuclear vacuole.

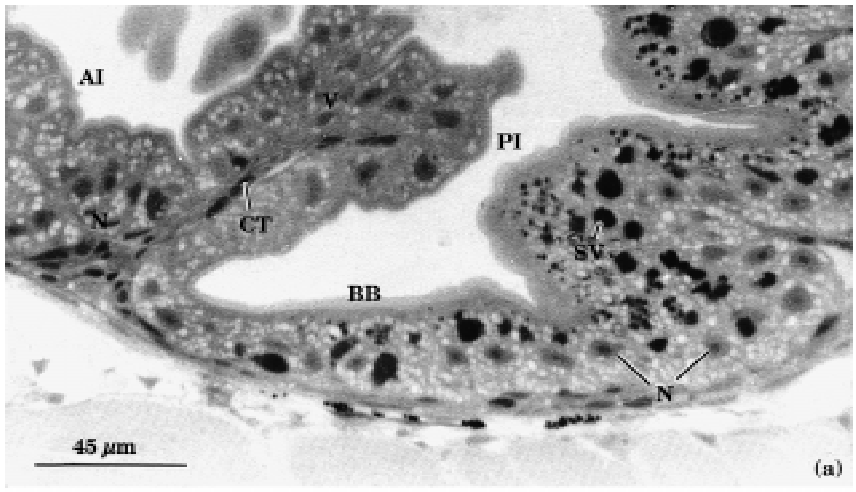
AI
V
PI
N
CT
SV
BB
N
45 μm
(a)

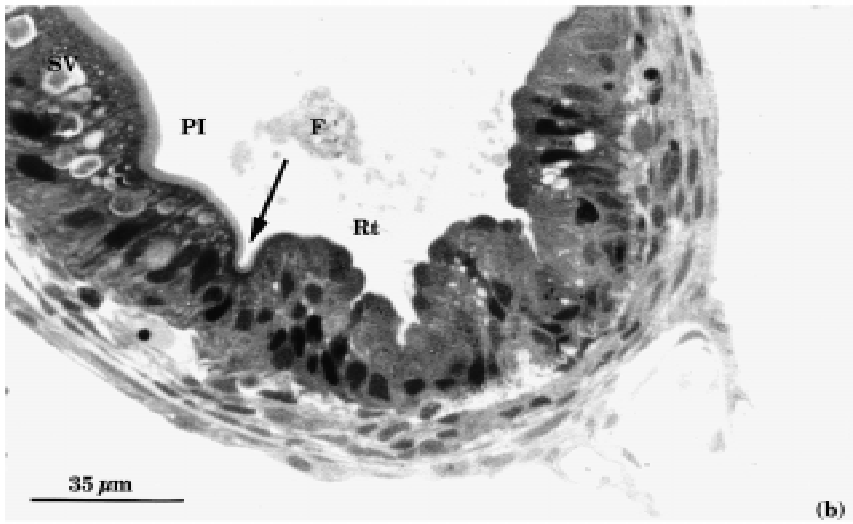
SV
PI
F
Rt
35 μm
(b)

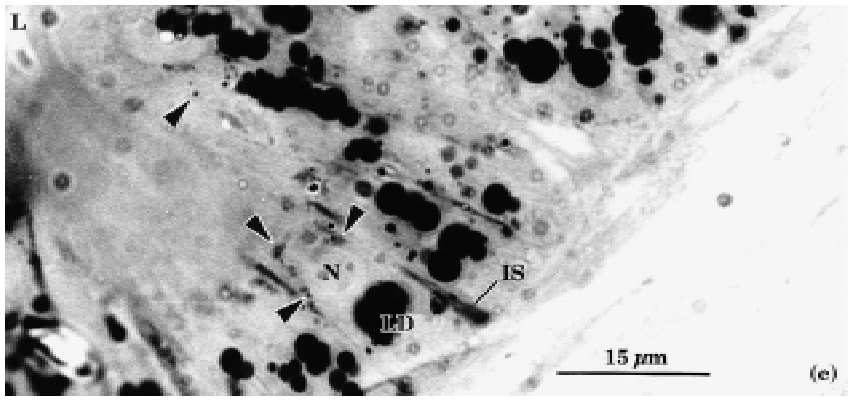
L
N
IS
ED
15 μm
(c)

Specimens were caught directly from the tanks and transported to the laboratory in glass beakers. The total time from capture of the samples to histological preparation varied from 1 to 2 h.

LIGHT MICROSCOPY

Since the larval body wall is transparent from D0 to D5, the gross gut anatomy can be examined directly on the light microscope by placing sea bream larvae on a cavity slide with a drop of water. For the histological study 10 specimens were sampled daily from D0 to D25. Prior to the fixation process, the larvae were transferred to a dish containing sea water placed on crushed ice. Whole larvae were fixed either in 10% formaldehyde in phosphate buffer (pH 7·2) or in Bouin's solution, dehydrated and embedded in paraffin wax. Sagittal and cross-sections (6–8 µm thick) were stained with haematoxylin–eosin. Some larvae were embedded in hydroxy-ethyl-methacrylate and 1-µm sections (cut on a Jung Supercut 2065 microtome) were stained with toluidine blue.

Lipid staining was performed following the method of Sire & Vernier (1980). In brief, semithin sections (1 µm) of larvae embedded in Spurr's resin (Spurr, 1969) were rinsed for 20 min in a solution containing 5% H_2O_2, then rinsed for 5 min in distilled water and treated with an alcohol solution of Sudan Black B for 45 min at 60° C. Then they were rinsed in 70% alcohol, washed in tap water, differentiated in 95% alcohol, and mounted in Canada balsam without counterstaining.

ELECTRON MICROSCOPY

Five individuals were sampled daily from D0 to D25. Whole larvae were fixed in 2·5% glutaraldehyde in 0·1 M sodium cacodylate buffer (pH 7·2) containing 3·5% sucrose at 4° C. After 30 min, the samples were transferred to a cavity slide placed on crushed ice and the tail was removed under the dissecting microscope in larvae from D0 to D10 to facilitate infiltration of the fixative. The tail and the head were cut in larvae from D11 to D20, and in larvae older than D20 various sections (1 mm long) of the intestinal region were cut. Following a total fixation time of ~3 h, the samples were rinsed in cacodylate buffer and post-fixed in 1% osmium tetroxide in cacodylate buffer, then dehydrated in a graded series of acetones, stained in bloc for 1 h in 1% uranyl acetate in 70% acetone, and embedded in Spurr's resin (Spurr, 1969). Semithin sections (0·5–1 µm) were stained with toluidine blue. Ultrathin sections were mounted on uncoated copper grids, stained with lead citrate and uranyl acetate and viewed in a JEOL 1200 EX transmission electron microscope operated at 80 kV.

Lipid cytochemistry was carried out on ultrathin sections by the OTO method (Seligman *et al.*, 1966).

ACID PHOSPHATASE CYTOCHEMISTRY

Whole D5 larvae were fixed for 2 h at 4° C in 2·5% glutaraldehyde in 0·1 M sodium cacodylate buffer (pH 7·2) containing 0·05% $CaCO_3$. After 30 min fixation, the gut was sliced in pieces of 1 mm. The cytochemical demonstration of acid phosphatase activity was carried out according to the method of Lewis & Knight (1977). The samples were incubated for 1 h in a medium consisting of 0·01 beta-glycerophosphate in 0·2 M acetate buffer (pH 5) containing 0·004 M lead nitrate. Control samples were incubated in a medium lacking the substrate (beta-glycerophosphate). After washing in cacodylate buffer, all the samples were post-fixed in 1% osmium tetroxide and processed for electron microscopy as described above. Samples were embedded in Epon 812. Ultrathin sections were examined without counterstaining.

RESULTS

LIGHT MICROSCOPY

At hatching [Fig. 1(a)], the alimentary canal of the sea bream is a more or less straight tube closed at both ends. The gut is lined by a simple columnar or pyramidal epithelium that lies on a layer of spindle-shaped cells. The urinary bladder anlage opens to the digestive tract [Fig. 1(b)] until D3, when the urinary

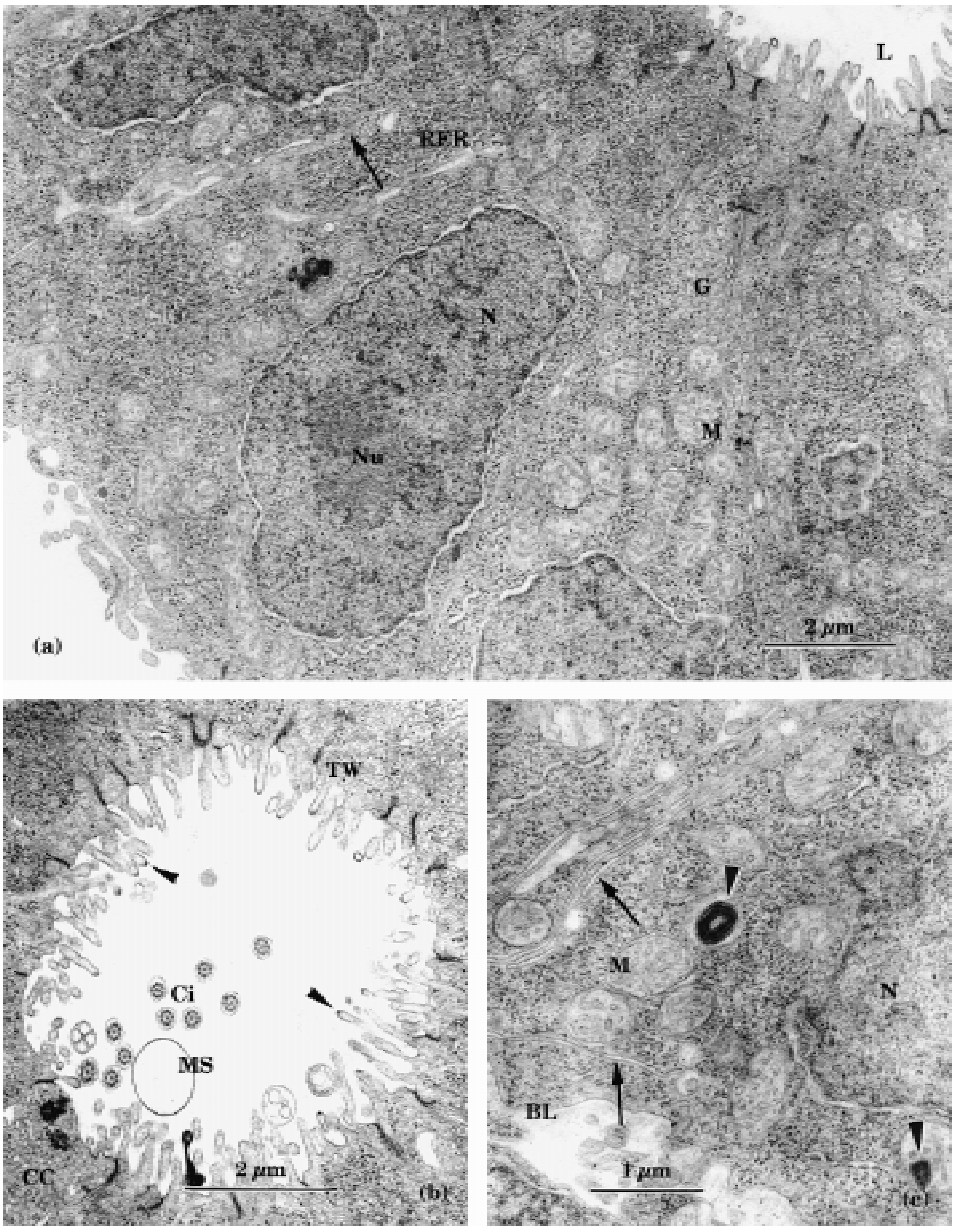

FIG. 3. Transmission electron microscopy (TEM). Midgut, endotrophic phase (D0). Cross-section. (a) Lamellar structures arising from the lateral membrane (→). Subepithelial tissue and basal lamina are not present. (b) Some microvilli show apical caps (►). (c) Lamellar structures (→) in the basal cytoplasm. Pseudomyelinic figures (►) are seen in the matrix of mitochondria. BL, Basal lamina; CC, ciliated cell; Ci, cilia; G, Golgi complex; L, lumen; M, mitochondrion; MS, membranous structures; N, nuclei; Nu, nucleolus; RER, rough endoplasmic reticulum; TW, terminal web.

canal detaches from the digestive tract and opens separately caudal to the anus. The anus opens by D1 [Fig. 1(b)], and the mouth by D3. During the study period, the stomach was not functional, since no gastric glands were developed.

Midgut

The midgut or anterior intestine anlage represents the longest segment of the gut. At D1 the midgut starts to coil to form a loop finally at D3. In D2 larvae, the rostral portion bends towards the ventral wall of the body and its lumen widens. The pancreatic (Wirsung) and bile (choledocus) ducts merge with the gut between the foregut and midgut [Fig. 1(c) and (d)]. At D3, the different areas of the digestive tract may be distinguished easily, and the anterior and posterior intestine are separated by the intestinal valve [Fig. 1(e)], the axis of which has been invaded by connective tissue.

Larvae first ingest food at D4. The rostral portion of the anterior intestine is dilated and small transversal folds are formed. From D4 to D15, small (<1 μm) lipid droplets (LD) are found in some cells. With the onset of *Artemia* feeding (D15), many large (>5 μm) LD appear in anterior enterocytes, mainly in the infranuclear cytoplasm. Small sudanophilic inclusions are found also in the apical cytoplasm, in the perinuclear region and in the intercellular spaces after D15 [Fig. 2(c)].

Hindgut

At hatching, the hindgut or posterior intestine anlage bends down from the posterior curvature of the gut [Fig. 1(a)]. At D4 some individuals show supranuclear vacuoles (SNV) in the posterior enterocytes. From D5, all larvae containing food in the gut show one or more giant SNVs (∼10 μm in diameter) per cell. During the endo-exotrophic phase (D4–D10), the intestinal valve acquires the definitive funnel-like shape that is observed in adults (Cataldi *et al.*, 1987). The intestinal valve lacks LD and SNV [Fig. 2(a)].

The posterior intestine is shorter than the anterior intestine and develops longitudinal folds. Lipid inclusions are rare. The most striking feature of posterior enterocytes is the presence of SNV throughout the exotrophic phase [Fig. 2(a) and (b)].

Rectum

The rectal anlage shortens gradually throughout the endotrophic phase [Fig. 1(a) and (b)] to become reduced to a short caudal segment (rectum) at the end of the endotrophic phase (D3) [Fig. 1(e)]. The rectum is the shorter segment of the intestine and usually shows no SNV or lipid inclusions [Fig. 2(b)].

ELECTRON MICROSCOPY

The presumptive intestine is lined by a simple columnar or pyramidal epithelium (∼15 × 5 μm). Four cell types constitute the gut epithelium: (1) non-ciliated epithelial cells, (2) ciliated epithelial cells, (3) leucocyte-like cells, and (4) enteroendocrine cells. At hatching, the gut lumen (∼5 μm in diameter) contains cilia that are more numerous in the transition between the hindgut and the rostral rectal anlage. Membranous structures sometimes fill the lumen from D0 to D2. At D1 and D2 the epithelium height increases (∼20 × 7 μm) and the lumen widens (∼10 μm in diameter). When the late endotrophic phase begins (D3), four to six tight folds can be seen in cross-sections of the midgut and cilia and membranous structures are no longer found in the lumen. The cells are now

typically columnar with a height ranging between 4 and 25 μm. The epithelial cells elongate from 25 μm (D4) to 40 μm (D25) in maximum length.

Midgut epithelium

At hatching, the epithelial non-ciliated cells display short (<1 μm in length) irregularly packed apical microvilli, some of which end in an electron-dense cap [Fig. 3(a) and (b)]. The voluminous euchromatinic nuclei contain one prominent central nucleolus [Fig. 3(a)] and are located in mid- or basal parts of the cells. The Golgi complex lies above the nucleus and the small size and low number of the associated vesicles appear to indicate poor activity [Fig. 3(a)]. The mitochondria are rounded or oval with electron-lucent matrices [Fig. 3(a)], some of them containing pseudomyelinic figures [Fig. 3(c)]. Cisternae of the endoplasmic reticulum (ER) are loose and scarce [Fig. 3(a)]. Lamellar structures are not well developed at hatching and, when present, are found mainly in the infranuclear cytoplasm [Fig. 3(c)]. The ciliated cells show cilia that run parallel to the lumen longitudinal axis. They are inserted between non-ciliated cells and are similar to them in morphology. However, they exhibit a lower number of microvilli and possess apical centrioles [Fig. 3(b)]. The ciliated cells disappear from D3 on. At hatching, two enteroendocrine cells were found in the midgut. They have round secretory granules (100–150 nm in diameter). The frequency of these cells remained very low throughout the endotrophic phase. They have been observed always to rest on the basal lamina and not to connect with the gut lumen. Infiltrated lymphocyte-like cells can also be found in the epithelium.

At D1, microvilli are more abundant and larger (1·5 μm) in the non-ciliated epithelial cells [Fig. 4(a)]. Apical plasma membrane invaginations and vesicles are rare [Fig. 4(b)]. Lamellar structures begin to associate with mitochondria in the basal cytoplasm [Fig. 4(c)]. At D2, microvilli are packed tightly and reach their maximum length (2 μm). Elements of the rough endoplasmic reticulum (RER) begin to arrange as stacks of two to three cisternae around the nucleus.

At D3 and D4 (late endotrophic phase) elongate large mitochondria are scattered throughout the cytoplasm of anterior enterocytes. Lysosomes, small (<1 μm) lipid droplets (LD) and vesicles of heterogeneous contents are seen [Fig. 5(a)]. The Golgi complex [Fig. 5(a)] and ER [Fig. 5(c)] show small (∼40 nm in diameter) LP. Intercellular spaces accumulate LP [Fig. 5(c)] and some of them are observed sometimes between the basal membrane and the basal lamina in close contact with lamellar structures [Fig. 5(d)]. The lamellar structures show a variable degree of development. They are especially abundant in the basal cytoplasm where large amounts of them constitute a basal labyrinth in some cells [Fig. 5(b)].

From D4 to D10 (endo-exotrophic phase), the ER cisternae increase in number mainly in the supranuclear cytoplasm. Mitochondria accumulate in the infranuclear cytoplasm, where they associate with lamellar structures. LP are observed within the Golgi complex and ER. LD are rare, and <1 μm in diameter.

When the exotrophic phase begins (D10), lysosomes and autophagic vacuoles are numerous [Fig. 6(a) and (b)]. The Golgi complex [Fig. 7(a)] and ER [Fig. 6(b)] are filled with LP (≤100 nm in diameter). Smooth vesicles and vacuoles containing LP are occasionally observed distant from the Golgi complex.

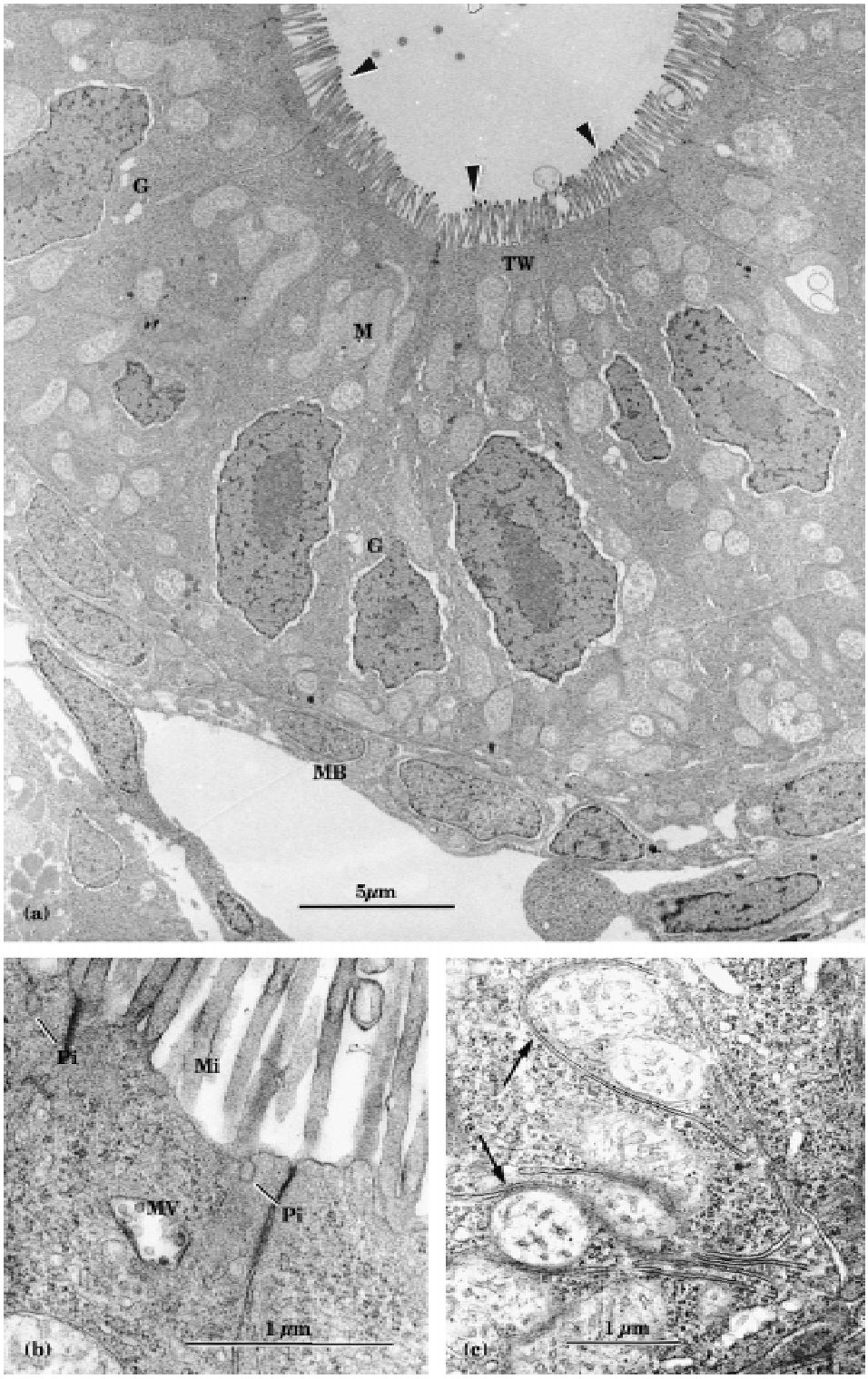
G
TW
M
G
MB
5μm
(a)
Pi
Mi
MV
Pi
1 μm
(b)
1 μm
(c)

Cisternae of the ER are sometimes observed in fusion with the lateral membrane and lamellar structures. Mitochondria accumulate in the basal cytoplasm [Fig. 6(a)] and are associated with lamellar structures. LD >5 μm in diameter appear in the infranuclear cytoplasm of some cells at the onset of *Artemia* feeding (D14) [Fig. 7(b)], though in the same region other cells may be almost devoid of LD. A massive accumulation of LD and LP (steatosis) may be observed in enterocytes. Intercellular spaces exhibit abundant LP.

Enteroendocrine cells increase their number in the exotrophic phase. After the onset of the exotrophic phase, the apical surface of most enteroendocrine cells is open to the gut lumen [Fig. 6(a)]. Infiltrated leucocyte-like cells are usually located over the basal lamina. Goblet cells appear from D12.

Hindgut epithelium

At hatching, structural differences occur between the midgut and hindgut non-ciliated cells. The hindgut cells are larger and their microvilli longer, more numerous, regularly packed and most of them bear an electron-dense cap. In contrast to midgut cells, invaginations of the apical plasma membrane and vesicles can be observed. Elongate mitochondria are common. Primary lysosomes are more numerous and lamellar structures more developed than in midgut cells.

In D1 larvae, invaginations of the apical membrane are more extensive. In the apical cytoplasm of D2 larvae pinocytic invaginations, vesicles and multivesicular bodies are numerous (Fig. 8). Small (<1 μm) LD are found in the basal cytoplasm.

Before mouth opening (D2–D3), a tubulovesicular system (TVS) has developed in the terminal web of posterior enterocytes. Endosomes ($\leq$1 μm in diameter) are numerous in the supranuclear cytoplasm [Fig. 9(a)]. Primary and secondary lysosomes are observed occasionally. ER cisternae, scarce during the early endotrophic phase, are now widespread. The nuclei are located mainly at the cell base, their profiles are more irregular than those of the midgut cells, and occasionally show indentations. Some cells display membrane-bound supranuclear polymorphic inclusions with a diverse degree of electron density [Fig. 9(a)]. The Golgi complex is less developed than in midgut cells and occasionally contains LP. Lamellar structures are more developed than in midgut cells and sometimes show terminal dilations [Fig. 9(b)]. Small LD (less than 0·5 μm in diameter) are seen in the basal cytoplasm [Fig. 9(c)].

At the onset of the endo-exotrophic phase (D4) (Fig. 10), the apical endocytic complex (pinocytic vesicles, TVS and endosomes) is well developed. Endosomes show electron dense amorphous contents, and their size increases towards the nucleus. SNV can reach up to 5 μm in diameter. Primary lysosomes measuring $\simeq$1 μm in diameter are found in the supranuclear cytoplasm. The nucleus has an uneven profile, and is sometimes deformed by the SNV (Fig. 10). From D5 onwards, the SNV grow to reach >10 μm.

FIG. 4. TEM. Midgut, endotrophic phase (D1). Cross-section. (a) Microvilli (►) are more numerous and larger than in D0. A layer of myoblasts (MB) underlies the epithelium. (b) Pinocytic invaginations (Pi) in the apical cytoplasm. (c) Association of lamellar structures (→) with mitochondria in the basal cytoplasm. G, Golgi complex; M, mitochondrion; Mi, microvilli; MV, multivesicular body; TW, terminal web.

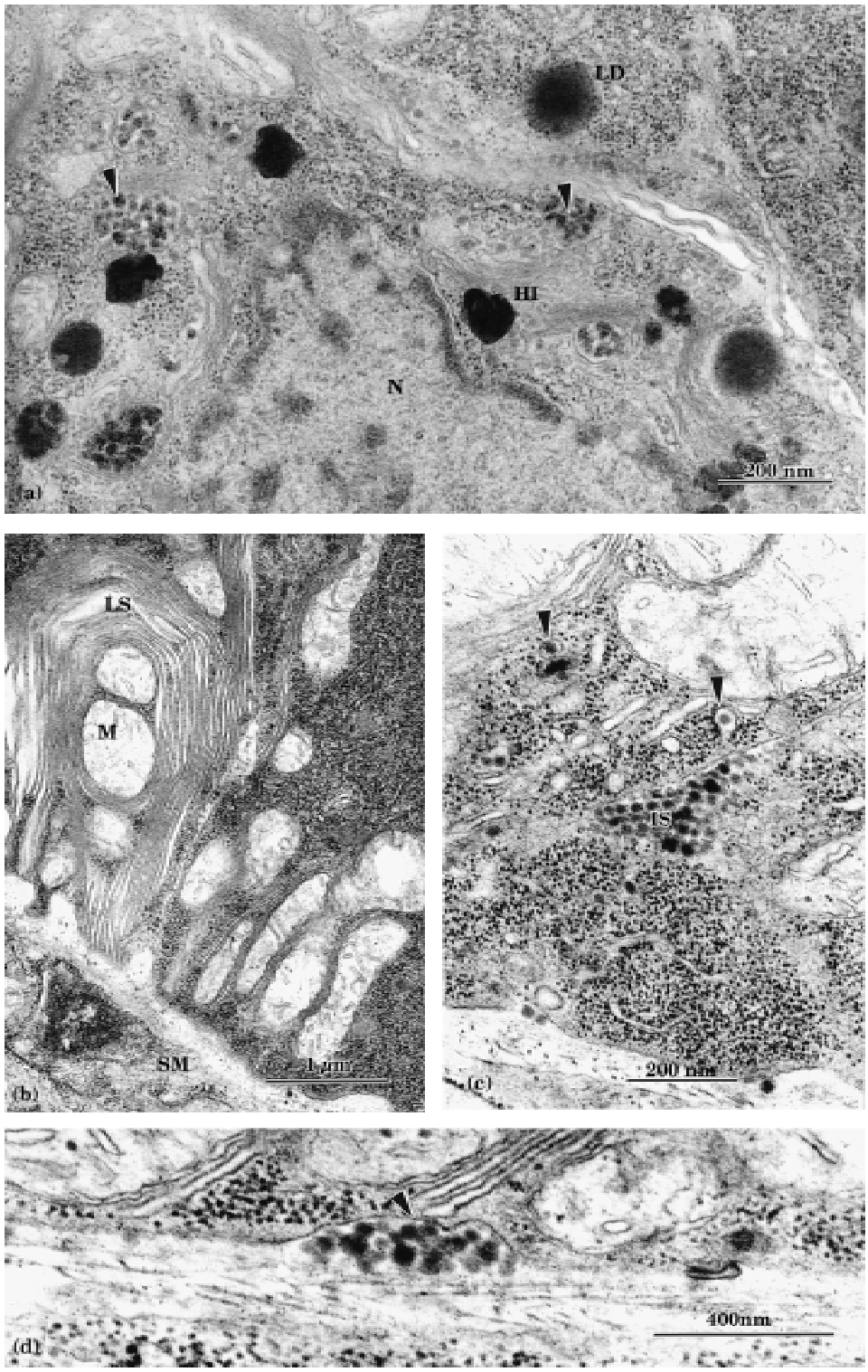
LD
HI
N
200 nm
(a)
LS
M
SM
1 µm
(b)
IS
200 nm
(c)
400nm
(d)

At the onset of the exotrophic phase (D10), the ER is not as developed as in anterior enterocytes and usually surrounds the nucleus. The supranuclear cytoplasm is virtually occupied by one or more SNV [Fig. 11(a)]. Numerous smaller autophagic vacuoles are also found. The content of the SNV is very heterogeneous (amorphous material, remnants of organelles, pseudomyelinic figures, and membranous structures). Fusion between SNV is usually observed [Fig. 11(a)]. Primary lysosomes can be found in fusion with the SNV [Fig. 11(a)], indicating the delivery of hydrolytic enzymes. The Golgi complex is well developed and usually lies around the SNV near the lateral plasma membrane [Fig. 11(b)]. Some specimens show LP in the Golgi complex [Fig. 11(b)], ER [Fig. 11(c)] and dilations of lamellar structures. As in the anterior enterocytes, connections of the ER with the lateral plasma membrane [Fig. 11(c)] and lamellar structures are observed. Intercellular spaces accumulate large amounts of LP (up to 100 nm in diameter) [Fig. 11(b) and (c)], some of them reaching 500 nm in diameter. Large LD are not present in the posterior enterocytes.

Enteroendocrine cells are common between enterocytes. Macrophages and lymphocyte-like cells are more abundant in the hindgut epithelium than in the midgut. Two rodlet cells were observed from D20 in the posterior intestine. They showed a thick fibrillar capsule with thin and thick filaments. However, no typical electron dense granules where observed in the cytoplasm. These features are coincident with the observation of Smith *et al.* (1995) on incompletely developed rodlet cells in the vascular system of the angelfish *Pterophyllum scalare scalare* (Lichtenstein). No goblet cells were seen in the posterior intestine.

Rectal epithelium

At hatching, the proximal rectum is lined by a simple columnar epithelium similar to that of the hindgut, though it exhibits distinct features. The apical membrane shows small cytoplasmic projections. In the apical cytoplasm, one or several centrioles are found commonly [Fig. 12(a)]. ER and lamellar structures are scarce. When the late endotrophic phase begins, the proximal rectum is lined by a simple columnar epithelium with a brush border [Fig. 12(b)] similar to that of the hindgut. The height and number of microvilli decrease towards the anus. The elongate nuclei usually exhibit indentations [Fig. 12(b)] and nucleoli are observed exceptionally. The distal rectum is lined by a cubical epithelium. The apical cytoplasmic projections disappear close to the anus [Fig. 12(c)]. The nuclei are about one-third of the cell volume, have an irregular shape and exhibit deep indentations. Nucleoli are very scarce. The Golgi complex is located in the supranuclear cytoplasm [Fig. 12(c)], the ER is scarce and lamellar structures have not been found in these cells. The ultrastructural features of this part of the rectum are retained throughout the endotrophic phase.

At the onset of exogenous feeding, some proximal rectal cells show apical invaginations, lysosomes and small (<1 μm) SNV with heterogeneous content, although no extensive TVS has been observed [Fig. 13(a)]. Cytoplasmic organelles

FIG. 5. TEM. Midgut, endotrophic phase (D3, D4). Cross section. (a) D3. LP (►) are found inside the Golgi complex. (b) D3. Basal cytoplasm of two enterocytes showing lamellar structures (LS) and mitochondria (M). (c) D4. LP (►) in the basal ER and intercellular space (IS). (d) D4. Extracellular LP (►) in close contact with lamellar structures. HI, Heterogeneous inclusion; LD, lipid droplet; N, nucleus; SM, smooth muscle cell.

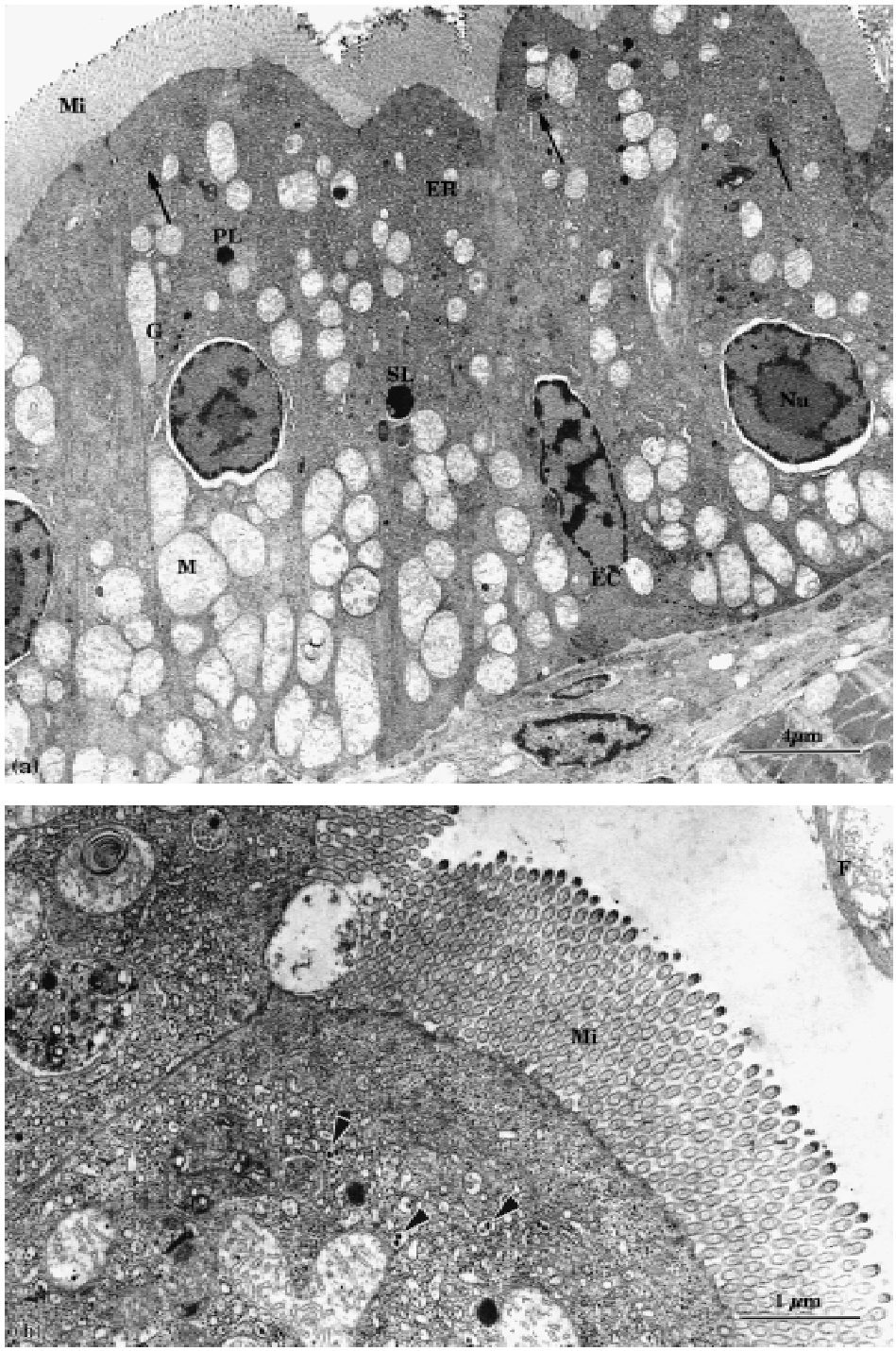

FIG. 6. TEM. Midgut, exotrophic phase (D12). Longitudinal section. (a) The endoplasmic reticulum (ER) predominates in the supranuclear cytoplasm, and mitochondria (M) are preferentially located at the infranuclear cytoplasm. Autophagic vacuoles (→) are numerous in the supranuclear cytoplasm. (b) LP (►) in the endoplasmic reticulum. EC, Enteroendocrine cell; G, Golgi complex; Mi, microvilli; Nu, nucleolus; PL, primary lysosome; SL, secondary lysosome.

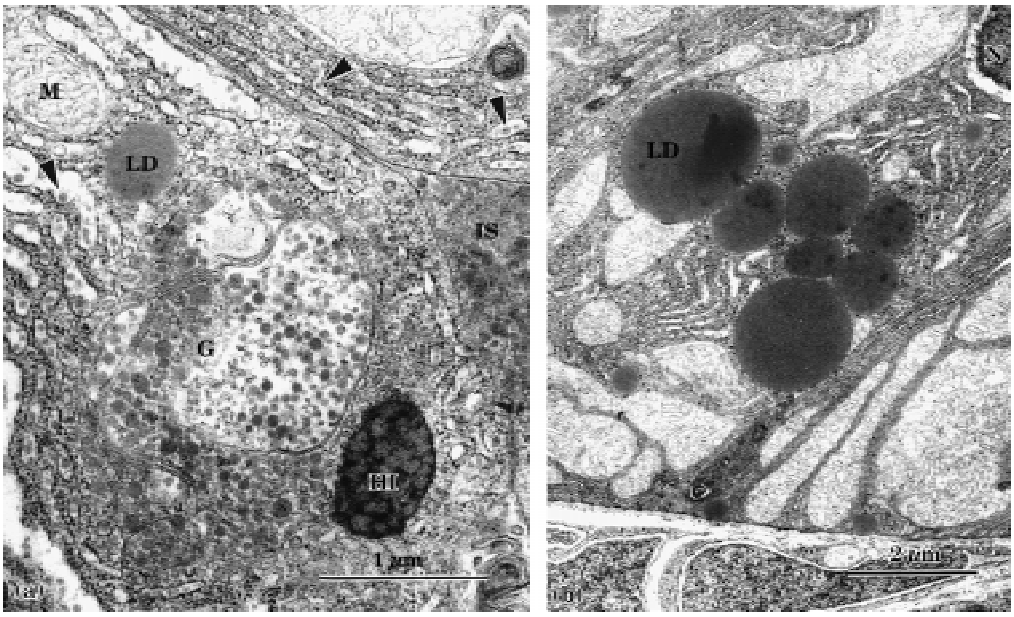

FIG. 7. TEM. Midgut, exotrophic phase (D20). Cross-section. (a) Golgi region. LP are numerous in the Golgi complex (G), in the RER (►) and intercellular spaces (IS). (b) LD in the infranuclear cytoplasm. HI, Heterogeneous inclusion; LD, lipid droplet; M, mitochondrion; N, nucleus.

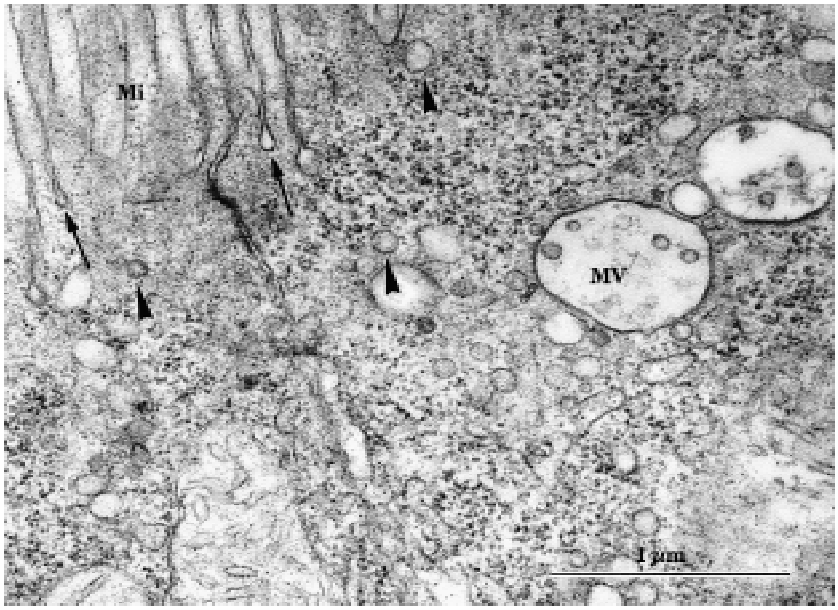

FIG. 8. TEM. Hindgut, endotrophic phase (D2). Cross-section. Pinocytic invaginations (→) and vesicles (►) are numerous. Mi, Microvilli; MV, multivesicular body.

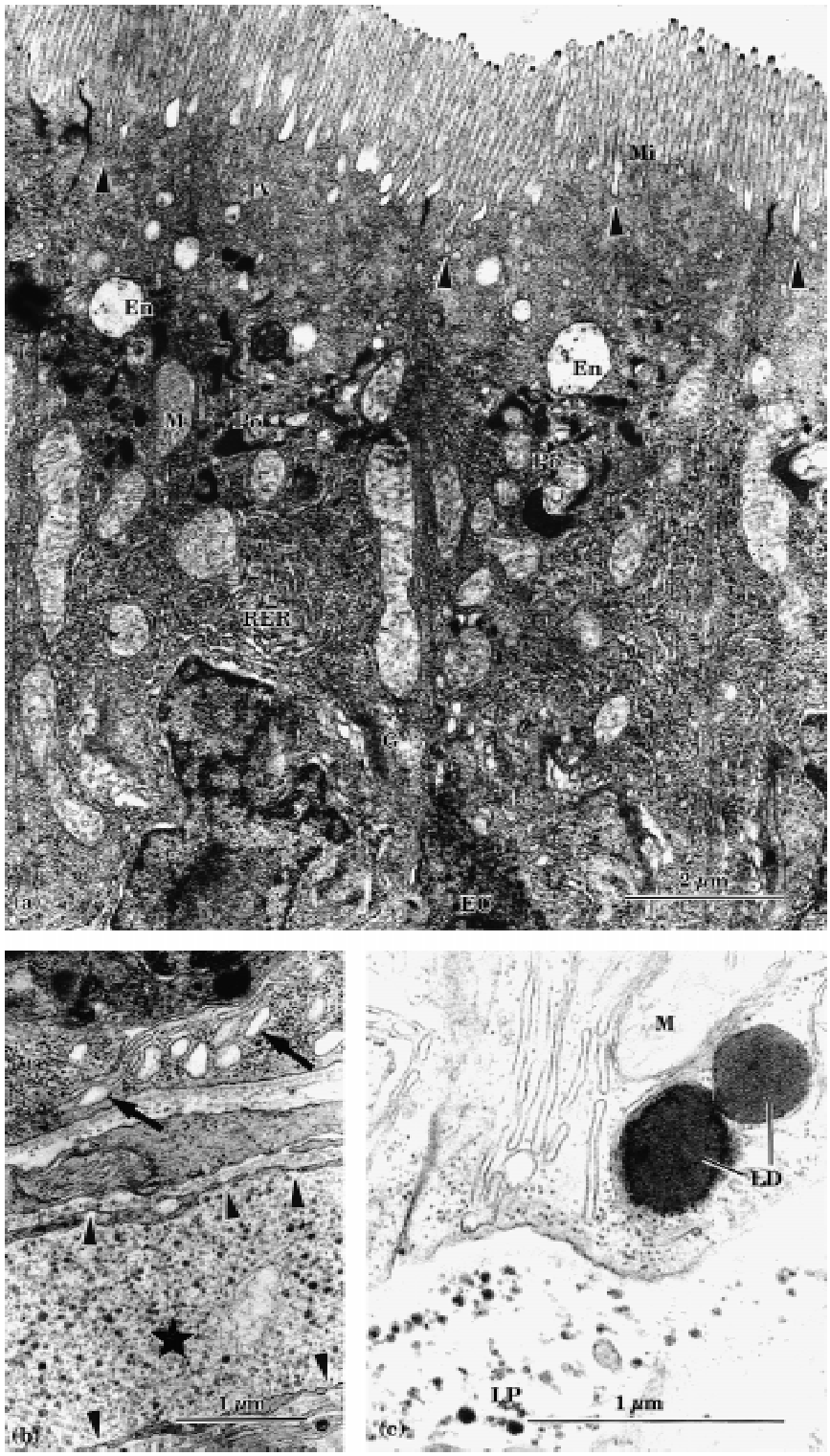
Mi
En
En
M
RER
G
2 µm
EC
1 µm
(b)
M
LD
LP
1 µm
(c)

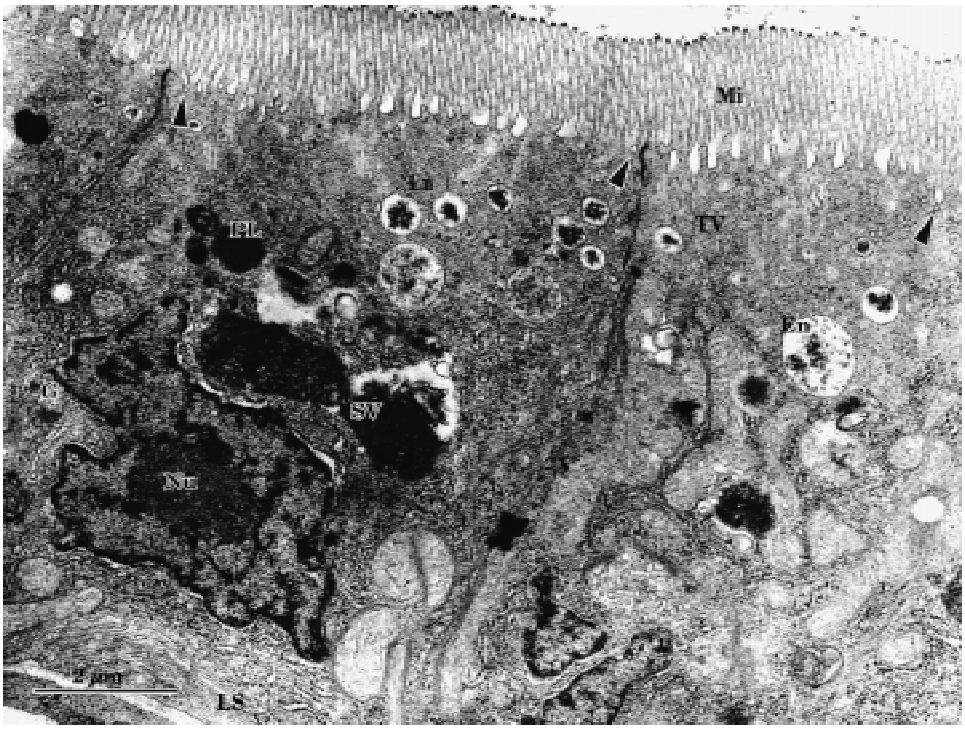

FIG. 10. TEM. Hindgut, endo-exotrophic phase (D4). Longitudinal section. Pinocytosis is conspicuous (►). Endosomes (En) show an electron-dense content and their diameter increases as they approach the nucleus. The supranuclear vacuole (SV) has a heterogeneous content. G, Golgi complex; LS, lamellar structures; Mi, microvilli: Nu, nucleolus; PL, primary lysosome; TV, tubulovesicular system.

are less abundant than in the other intestinal segments. Small LD are sometimes present in rectal cells [Fig. 13(a)], and ER and the Golgi complex may exhibit a few LP within their cisternae. As in the other intestinal segments, smooth vacuoles that coalesce with the lateral plasma membrane are observed to contain LP [Fig. 13(b)]. The intercellular spaces accumulate large amounts of LP [Fig. 13(b)]. Enteroendocrine and leucocyte-like cells are found also in the rectal epithelium.

Subepithelial tissue

The morphology of the subepithelial tissue is similar all along the presumptive intestine during the studied period. It is not continuous along the entire gut at hatching [Figs 3(a) and 12(c)]. In the zones where it has developed [Fig. 4(a)], it consists of a layer of one to three spindle-shaped myoblasts with voluminous nuclei. Mitochondria are moderately abundant, and ribosomes and ER scarce.

FIG. 9. TEM. Hindgut, endotrophic phase (D4). Cross-section. (a) Pinocytosis is extensive (►). A tubulovesicular complex (TV) has developed in the apical cytoplasm. Endosomes (En) and polymorphic inclusions (Po) are found below. (b) Vessel of the circulatory system (★) showing the fenestrated endothelium (►) and LP in the lumen. Dilations of lamellar structures (→) are found in the infranuclear cytoplasm. (c) Basal cytoplasm. The contrast of lipid droplets (LD) and lipoprotein particles (LP) is enhanced when stained by the OTO method. EC, Enteroendocrine cell; G, Golgi complex; M, mitochondrion; Mi, microvilli; RER, rough endoplasmic reticulum.

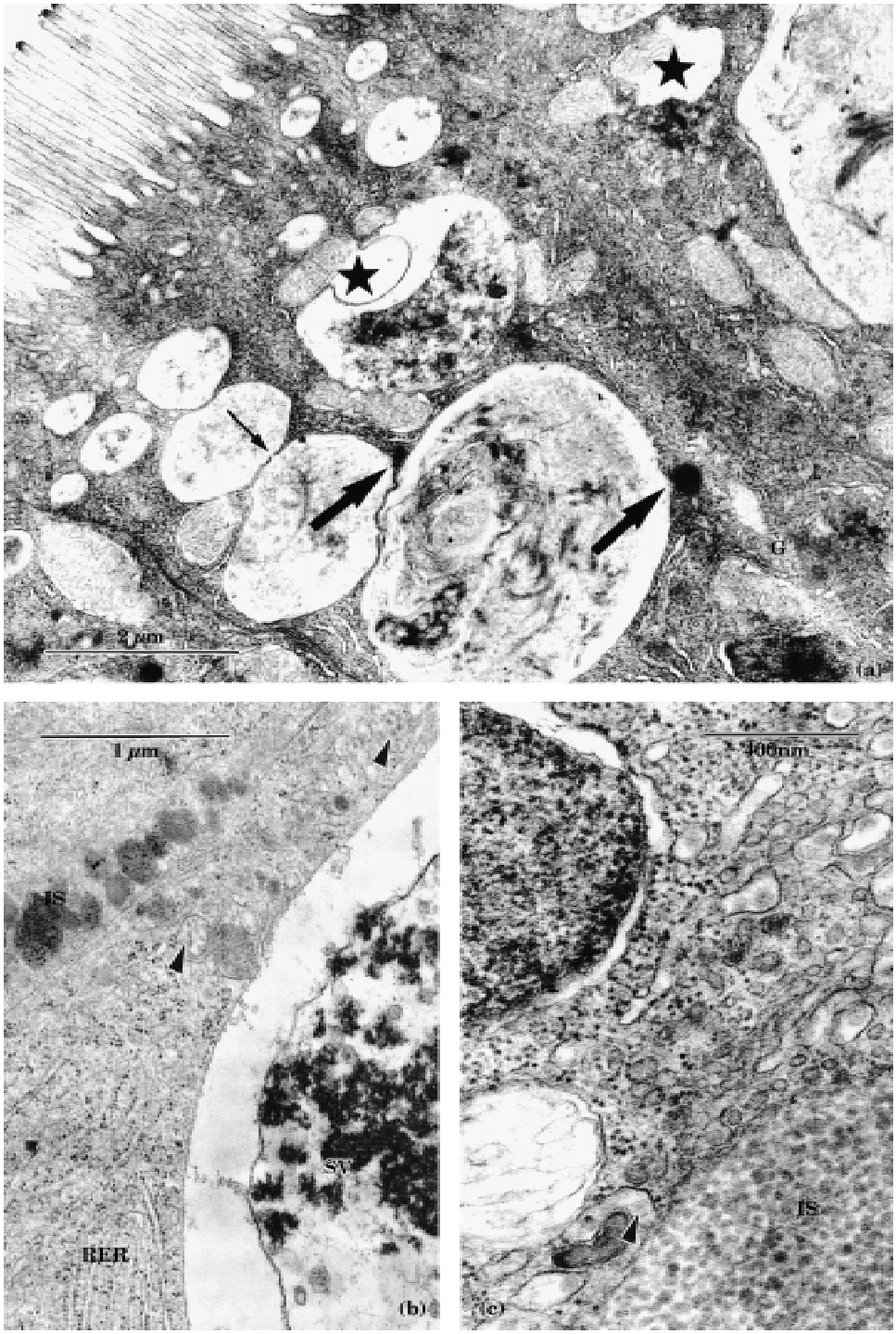
L
G
2 μm
(a)
1 μm
IS
SV
RER
(b)
100nm
IS
(c)

The Golgi complex is located close to the nucleus. These cells show cytoplasmic extensions that sometimes overlap neighbouring cells [Fig. 4(a)]. During the late endotrophic phase (D3), they differentiate into smooth muscle cells [Fig. 5(b)], which represent the main cell type of the subepithelial tissue. Vessels of the circulatory system appear at this stage. The fenestrated endothelium (pores $\leq$100 nm in diameter) [Fig. 9(b)] is very thin, except in the nuclear region. The subepithelial tissue regularly underlies the epithelium [Fig. 6(a)] during the exotrophic phase, though it is possible to find areas devoid of it, even in D15 larvae. Lymphocyte-like, fibroblast-like and macrophage-like cells are observed occasionally. LP accumulate first in the gut at D3. They can be found in the circulatory vessels (lumen and vesicles of endothelial cells), interstitial spaces, vesicles of fibroblast-like cells, vesicles of smooth muscle cells and intercellular spaces of the gut. From D5, LP are less abundant in the subepithelial tissue. During the exotrophic phase the amount of LP increases again [Fig. 13(c)].

ACID PHOSPHATASE CYTOCHEMISTRY

Acid phosphatase activity was studied in D5 anterior and posterior intestinal cells. In the anterior enterocytes, the enzymatic activity was detected in the brush border, lysosomes and in the Golgi complex. In posterior enterocytes phosphatase activity was observed in the brush border [Fig. 14(a)], primary lysosomes [Fig. 14(b) and (c)], Golgi complex [Fig. 14(c)] and some SNV [Fig. 14(c)]. TVS and endosomes did not show acid phosphatase reaction [Fig. 14(b)]. Some primary lysosomes were observed in coalescence with apical endosomes to form secondary lysosomes [Fig. 14(b)]. Unspecific staining was observed in the nucleus, lamellar structures, basal lamina and interstitial spaces of the subepithelial tissue.

DISCUSSION

As in other teleost species (Stroband & Dabrowski, 1979; Cousin & Baudin-Laurencin, 1985; Boulhic & Gabaudan, 1992; Bisbal & Bengtson, 1995), the larval gut of the sea bream is undifferentiated and immature at hatching. However, it is already possible to tell regional differences between the presumptive enterocytes: the hindgut cells are more developed than midgut cells, whereas most rectal cells show no clear signs of cellular differentiation. As observed in the halibut *Hippoglossus hippoglossus* L. (Kjørsvik & Reiersen, 1992), the cytoplasmic organelles are more abundant in the hindgut.

During the early endotrophic phase (D0–D2) major changes occur in the sea bream digestive system. The anus and mouth open, gut cells undergo a significant growth and exhibit an increased development of organelles and the intestinal valve is being formed. The first zymogen granules appear in exocrine pancreatic cells (Diaz *et al.*, 1992), the bile canaliculi develop, and glycogen synthesis starts in hepatoblasts (Guyot *et al.*, 1995). Finally, the liver and

FIG. 11. TEM. Hindgut, exotrophic phase (D25). Cross-section. (a) Two supranuclear vacuoles are connected at a point (→). Primary lysosomes are observed in fusion with supranuclear vacuoles (⟶). Remnants of organelles are engulfed into supranuclear vacuoles (★). (b) LP in the Golgi complex (►). Chylomicron-like particles are found in the intercellular space (IS). (c) RER cisterna containing LPs (►) in close association with the lateral plasma membrane. The intercellular space (IS) is filled with LP. G, Golgi complex; SV, supranuclear vacuole.

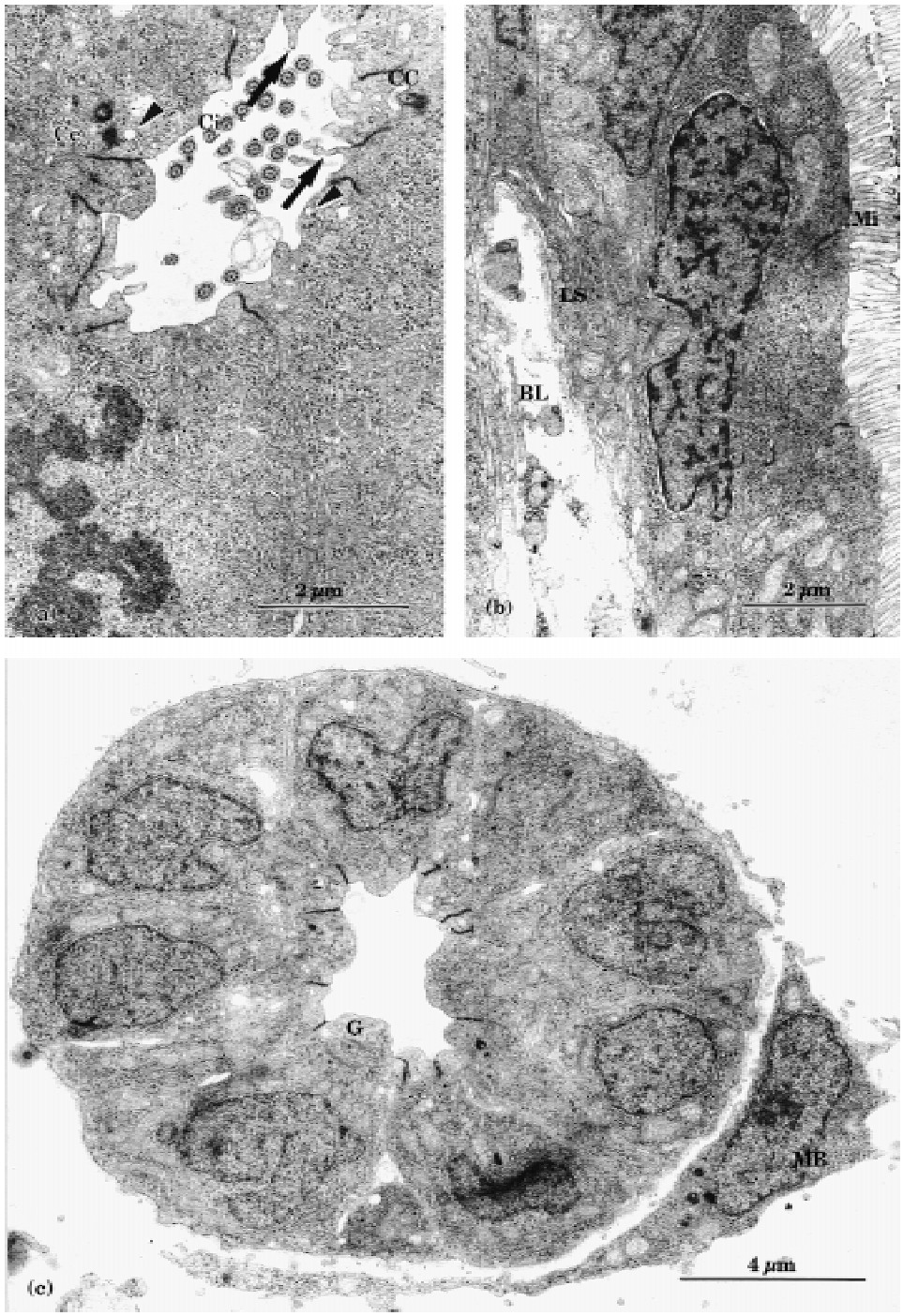

FIG. 12. TEM. Rectum, endotrophic phase (D0, D4). Cross-section. (a) Proximal rectum, D0. Note the projections of the apical membrane (→), some clear vesicles (►) and centrioles (Ce). (b) Proximal rectum, D4. (c) Distal rectum, D0. The epithelium is nearly cubical and the cells lack microvilli. No cilia are found in the lumen. The subepithelial tissue is not continuous. BL, Basal lamina; Ci, cilia; CC, ciliated cell; G, Golgi complex; LS, lamellar structures; MB, myoblast; Mi, microvilli.

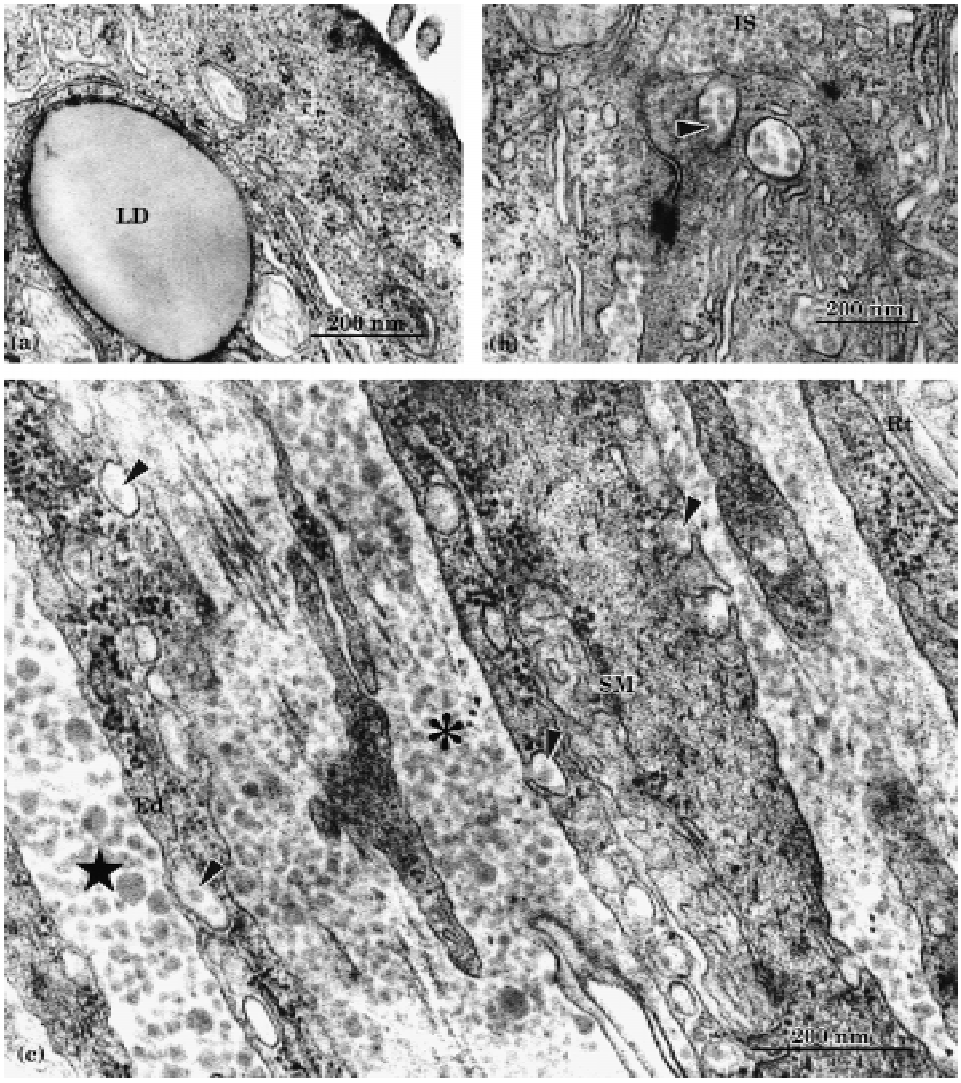

FIG. 13. TEM. Rectum, exotrophic phase (D25). Cross-section. (a) Lipid droplet (LD) in the apical cytoplasm of a distal rectal cell. (b) Smooth vesicle containing LP (►) in association with the lateral plasma membrane. (c) LP are found in the interstitial spaces of the subepithelial tissue (*) and vesicles (►) of smooth muscle cells (SM) and endothelial cells (Ed), and lumen of a circulatory vessel (★). IS, Intercellular space; Rt, rectal cell.

pancreas become connected with the gut, thus allowing the evacuation of bile salts and digestive enzymes. On the other hand, ultrastructural observations suggest pinocytic absorption in hindgut cells at D0, and histochemical tests demonstrated the presence of acid (D1) and alkaline (D2) phosphatase activities in the brush border of the sea bream gut (Calzada, 1996). Both morphological and histochemical observations suggest that early sea bream larvae possess digestive organs enabling digestion, absorption and metabolization of endogenous food. At the onset of the late endotrophic phase (D3), enterocytes are morphologically similar to those of adults (Elbal & Agulleiro, 1986).

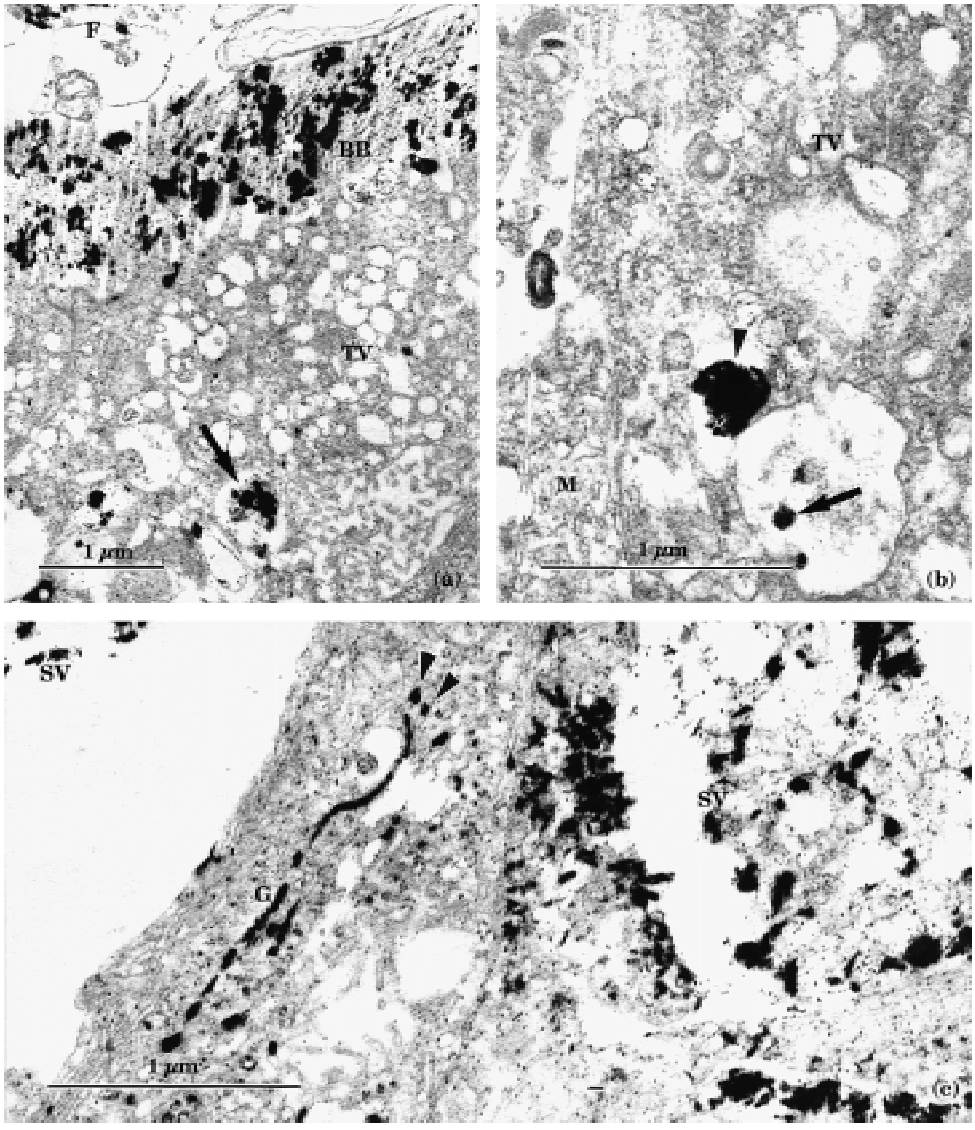

FIG. 14. Acid phosphatase cytochemistry. Hindgut (D5). Cross-section. (a) The reaction is detected in the brush border (BB) and in some apical vacuoles (→). The apical tubulovesicular system (TV) lacks acid phosphatase reaction. (b) A primary lysosome (►) is associated with an apical vacuole (→), both showing acid phosphatase activity. (c) Acid phosphatase activity is found in the supranuclear vacuoles (SV), Golgi complex (G) and primary lysosomes (►). F, Food; M, mitochondrion; TV, tubulovesicular system.

Sea bream yolksac larvae synthesize LP mainly in the periblast (Guyot *et al.*, 1993), and to a lesser extent in the liver (Guyot *et al.*, 1995). At D3, LP accumulate in the circulatory vessels and intercellular spaces of the gut. Although the present study shows that anterior enterocytes are involved in LP synthesis before mouth opening, the low diameter and number of LP do not account for the high accumulation mentioned above. After mouth opening, a decrease in the LP is observed in the sea bream gut circulatory vessels and

intercellular spaces. It is suggested that the gut LP reserves, originated mainly in the periblast, are being used for larval motility, since oil globule fatty acids are the primary metabolic fuel in sea bream larvae (Rønnstad *et al.*, 1994) and it is evident that an increase of energy requirements occurs during prey capture.

During the endo-exotrophic phase (D4–D10) the synthesis of LP is more conspicuous in the anterior enterocytes than in the endotrophic phase. As observed in adults of other species (Vernier & Sire, 1986; Deplano *et al.*, 1989), when the sea bream anterior enterocytes are absorbing lipids actively, the Golgi complex accumulates large amounts of LP and swells considerably. In the larval sea bream the synthesis of LP occurs in the ER, from where they can be released into the intercellular spaces and lamellar structures. As reported in the adult rainbow trout *Oncorhynchus mykiss* (Walbaum) (Vernier & Sire, 1986), the Golgi complex does not seem to be an obligatory step in the process of LP secretion by intestinal cells. Therefore, the traffic of LP from the enterocytes to the extracellular spaces may follow two alternative pathways: (a) direct exocytosis from the ER, and (b) via the Golgi complex, as occurs in mammals. At this stage, LD are small and scarce, in contrast to the observations of Diaz *et al.* (1997), who reported the presence of large LD and chylomicrons (LP up to 500 μm). Plausibly, such differences reflect the distinct lipid enrichment of rotifers provided in the diet. While the sea bream larvae used in this study were fed algae-enriched rotifers, those used by Diaz *et al.*, were fed cod liver oil-enriched rotifers. It is assumed that large LD and the size of the LP of anterior enterocytes is correlated with the nature of the dietary fatty acids (Bergot & Fléchon, 1970*a*,*b*; Sire & Vernier, 1981).

LD less than 5 μm proliferate in sea bream anterior intestine after feeding on *Artemia* nauplii (D15), probably due to the nature of the fatty acid contents of the diet. It has been shown that after supplying a lipid-rich diet, numerous LD appear in the cytoplasm of anterior enterocytes of larval and adult teleost species (Iwai, 1968; Bergot & Fléchon, 1970*b*; Noaillac-Depeyre & Gas, 1974, 1976, 1979, 1983; Sire & Vernier, 1981; Segner *et al.*, 1987*a*,*b*, 1993). Deplano *et al.* (1989) reported that LD were scarce, clear, small and homogeneous in the intestine of adult wild *Dicentrarchus labrax* (L.). However, intestinal steatosis was observed in specimens fed an artificial diet. Also a certain degree of steatosis was found in anterior enterocytes of *Artemia*-fed larvae, but no cell degeneration, as shown by Deplano *et al.* (1989).

It is generally assumed that lipid absorption takes place in the anterior intestine. However, this study found some specimens that exhibited LP synthesis in posterior enterocytes, and even in rectal cells. A few references show a restricted LP synthesis in posterior enterocytes (Stroband & Debets, 1978; Watanabe & Sawada, 1985; Deplano *et al.*, 1991*a*), but to our knowledge, rectal LP synthesis has not been documented.

The lamellar structures increase the membrane surface that is in contact with the extracellular spaces, probably facilitating LP transport. The involvement of these membrane infoldings in the transport of LP has been suggested by several authors (Bergot & Fléchon, 1970*a*; Noaillac-Depeyre & Gas, 1974, 1979, 1983; Deplano *et al.*, 1991*a*). They are closely associated with mitochondria in the basal cytoplasm. This is due probably to an increased demand of energy for osmoregulation processes, since the gut is the primary organ for absorbing water

to maintain water and ion balance in marine larval fishes (Tytler & Ireland, 1994). The morphological similarity between these structures and others described in kidney ducts (Calzada, 1996), oesophagus (Meister *et al.*, 1983) and gills (Pisam *et al.*, 1990) support the view that, apart from participating in lipid transport, the lamellar structures play a role in osmoregulation.

Before the onset of exogenous feeding, the posterior sea bream enterocytes differentiate an apical endocytic system. This complex enlarges throughout the exotrophic phase and the acid phosphatase reaction is detected in the primary lysosomes and SNV. Thus, the sea bream posterior enterocytes display the typical structure of cells involved in absorption and intracellular digestion of macromolecules (Iida & Yamamoto, 1985; Iida *et al.*, 1986). It has been shown that via the endocytic system, posterior enterocytes of teleost larvae take up intact macromolecules which may be degraded in the SNV (Watanabe, 1981, 1982, 1984*a*,*b*; Deplano *et al.*, 1991*b*; Otake *et al.*, 1995). In the present study, remnants of cytoplasmic organelles have been observed in the SNV, which suggest that, apart from the digestive role in degrading exogenous macromolecules, the SNV operate also as autophagic vacuoles.

In conclusion, in about 3 days, when the yolk reserves are almost exhausted (Mani-Ponset *et al.*, 1996), the gut of the sea bream develops from a relatively undifferentiated short tube at hatching to a complex tract before the onset of exogenous feeding. During the endotrophic phase LP are synthesized in the Golgi complex and ER anterior enterocytes from endogenous reserves (plasma fatty acids, bile salts, membranes and cells rejected into the lumen). Simultaneously, LP synthesized mainly in the periblast accumulate in the intestinal mucosa and will be used as an energy source after mouth opening, when the larvae are capturing prey actively. During the endo-exotrophic phase, the fatty acid contents provided by the alga *N. gaditana* (natural enrichment) (Mourente *et al.*, 1990), is probably correlated with the low number of small LD found in enterocytes. On the other hand, the onset of *Artemia* feeding (artificial enrichment) gives rise to large enterocytes containing LD and chylomicron-like particles in intercellular spaces. It is suggested that the increase of LD in anterior enterocytes and the presence of chylomicron-like particles in intercellular spaces are induced by excess lipid in the larval diet, which may in turn cause intestinal steatosis, as has been documented in the sea bass (Deplano *et al.*, 1989). To what extent steatosis may affect the larval production is still a question that remains unsolved. The posterior intestine is specialized in the absorption and intracellular digestion of macromolecules that have not been degraded totally in the lumen, because of a low acid protease activity (Moyano *et al.*, 1996). The absorption and intracellular breakdown of macromolecules in the posterior intestine would have an important nutritive function in agastric species and larvae, where the gastric glands are not developed.

The authors thank CUPIMAR, S.A. for providing the animals, and A. Santos for technical assistance.

References

Bergot, P. & Fléchon, J. E. (1970*a*). Forme et voie d'absorption intestinale des acides gras a chaîne longue chez la truite arc-en-ciel (*Salmo gairdneri* Rich.). I.—Lipides en particules. *Annales de Biologie animale, Biochimie et Biophysique* **10,** 459–472.

Bergot, P. & Fléchon, J. E. (1970*b*). Forme et voie d'absorption intestinale des acides gras a chaîne longue chez la truite arc-en-ciel (*Salmo gairdneri* Rich.). II.—Lipides ' étalés '. *Annales de Biologie animale, Biochimie et Biophysique* **10,** 473–480.

Bisbal, G. A. & Bengtson, D. A. (1995). Development of the digestive tract in larval summer flounder. *Journal of Fish Biology* **47,** 277–291.

Blaxter, H. H. S. (1988). Pattern and variety in development. In *Fish Physiology* Vol. XIA (Hoar W. S. & Randall D. J., eds), pp. 1–58. San Diego, CA: Academic Press.

Boulhic, M. & Gabaudan, J. (1992). Histological study of the organogenesis of the digestive system and swim bladder of the dover sole, *Solea solea* (Linnaeus, 1758). *Aquaculture* **47,** 305–319.

Calzada, A. (1996). Desarrollo postembrionario del intestino y órganos asociados de la dorada, *Sparus aurata* L., en cultivo. Estudio histológico y ultraestructural. PhD Thesis. University of Cádiz.

Cataldi, E., Cataudella, S., Monaco, G., Rossi, A. & Tancioni, L. (1987). A study of the histology and morphology of the digestive tract of the sea-bream, *Sparus aurata*. *Journal of Fish Biology* **30,** 135–145.

Connes, R. & Benhalima, K. (1983). Ultrastructure de l'intestine du loup *Dicentrarchus labrax* au cours du développement larvaire. *Bulletin de la Societé Zoologique de France* **109,** 19–33.

Cousin, J. B. C. & Baudin-Laurencin, F. (1985). Morphogénèse de l'appareil digestif et de la vessie gazeuse du turbot, *Scophthalmus maximus*, L. *Aquaculture* **47,** 305–319.

Deplano, M., Connes, R., Diaz, J. P. & Paris, J. (1989). Intestinal steatosis in the farm-reared sea bass, *Dicentrarchus labrax*. *Diseases of Aquatic Organisms* **6,** 121–130.

Deplano, M., Diaz, J. P., Connes, R., Kentouri-Divanach, M. & Cavalier, F. (1991*a*). Appearance of lipid-absorption capacities in larvae of the sea bass *Dicentrarchus labrax* during transition to the exotrophic phase. *Marine Biology* **108,** 361–371.

Deplano, M., Connes, R., Diaz, J. P. & Barnabé, G. (1991*b*). Variation in the absorption of macromolecular proteins in larvae of the sea bass *Dicentrarchus labrax* during transition to the exotrophic phase. *Marine Biology* **110,** 29–36.

Diaz, J. P., Carmona-Sepulveda, M. & Connes, R. (1992). L'organogenèse du pancréas exocrine chez la daurade (*Sparus aurata* L.). *Cahiers Agricultures* **1,** 101–108.

Diaz, J. P., Guyot, E., Vigier, S. & Connes, R. (1997). First event in lipid absorption during post-embryonic development of the anterior intestine in gilt-head sea bream. *Journal of Fish Biology* **51,** 180–192.

Elbal, M. T. & Agulleiro, B. (1986). A histochemical and ultrastructural study of the gut of *Sparus auratus* (Teleostei). *Journal of Submicroscopical Cytology* **18,** 335–347.

Fernández-Díaz, E., Pascual, E. & Yúfera, M. (1994). Feeding behaviour and prey size selection of gilthead seabream, *Sparus aurata*, larvae fed on inert and live food. *Marine Biology* **118,** 323–328.

Fyhn, H. J. (1989). First feeding of marine fish larvae: are free amino acids the source of energy? *Aquaculture* **80,** 111–120.

Guyot, E., Connes, R. & Diaz, J. P. (1993). Résorption des réserves vitellines et passage de l'endotrophie à l'exotrophie chez la larve de Daurade (*Sparus aurata*) norrie et à jeun. In *Production, Environment and Quality* (Barnabé, G. & Kestemont, P., eds). European Aquaculture Society Special Publication **18,** 213–226.

Guyot, E., Diaz, J. P. & Connes, R. (1995). Organogenesis of the liver in sea bream. *Journal of Fish Biology* **47,** 427–437.

Iida, H. & Yamamoto, Y. (1985). Intracellular transport of horseradish peroxidase in the absorptive cells of goldfish hindgut in vitro, with special reference to the cytoplasmic tubules. *Cell and Tissue Research* **240,** 553–560.

Iida, H., Shibata, Y. & Yamamoto, Y. (1986). The endosome-lysosome system in the absorptive cells of goldfish hindgut. *Cell and Tissue Research* **243,** 449–452.

Iwai, T. (1968). The comparative study of the digestive tract of teleost larvae—V. Fat absorption in the gut epithelium of goldfish larvae. *Bulletin of the Japanese Society of Scientific Fisheries* **34,** 973–978.

Kjørsvik, E. & Reiersen, A. L. (1992). Histomorphology of the early yolk-sac larvae of the Atlantic halibut (*Hippoglossus hippoglossus* L.)—an indication of the timing of functionality. *Journal of Fish Biology* **41,** 1–19.

Lewis, P. R. & Knight, D. P. (1977). Staining methods for sectioned material. In *Practical Methods in Electron Microscopy* Vol. 5, part I (Glauert, A. M., ed.), pp. 158–162. Amsterdam: North Holland Publishing Company.

Mani-Ponset, L., Guyot, E., Diaz, J. P. & Connes, R. (1996). Utilization of yolk reserves during post-embryonic development in three teleostean species: the sea bream *Sparus aurata*, the sea bass *Dicentrarchus labrax*, and the pike-perch *Stizostedion lucioperca*. *Marine Biology* **126,** 539–547.

Meister, M. F., Humbert, W., Kirsch, R. & Vivien-Roels, B. (1983). Structure and ultrastructure of the oesophagus in sea-water and fresh-water teleosts (Pisces). *Zoomorphology* **102,** 33–51.

Mourente, G. & Odriozola, J. M. (1990*a*). Effect of broodstock diets on total lipids and their fatty acid composition in eggs of gilthead sea bream (*Sparus aurata* L.) during yolksac stage. *Fish Physiology and Biochemistry* **8,** 93–101.

Mourente, G. & Odriozola, J. M. (1990*b*). Effect of broodstock diets on total lipids and their fatty acid composition of larvae of gilthead sea bream (*Sparus aurata* L.) during yolksac stage. *Fish Physiology and Biochemistry* **8,** 103–110.

Mourente, G., Lubián, L. M. & Odriozola, J. M. (1990). Total fatty acid composition as a taxonomic index of some marine microalgae used as food in marine aquaculture. *Hydrobiologia* **203,** 147–154.

Moyano, F. J., Díaz, M., Alarcón, F. J. & Sarasquete, M. C. (1996). Characterization of digestive enzyme activity during larval development of gilthead seabream (*Sparus aurata*). *Fish Physiology and Biochemistry* **15,** 121–130.

Noaillac-Depeyre, J. & Gas, N. (1974). Fat absorption by the enterocytes of the carp (*Cyprinus carpio* L.). *Cell and Tissue Research* **155,** 353–365.

Noaillac-Depeyre, J. & Gas, N. (1976). Electron microscopic study on gut epithelium of tench (*Tinca tinca* L.) with respect to its absorptive functions. *Tissue and Cell* **8,** 511–530.

Noaillac-Depeyre, J. & Gas, N. (1979). Structure and function of the intestinal epithelial cells in the perch (*Perca fluviatilis* L.). *Anatomical Record* **195,** 621–640.

Noaillac-Depeyre, J. & Gas, N. (1983). Étude cytophysiologique de l'epithélium intestinal du poisson-chat (*Ameiurus nebulosus* L.). *Canadian Journal of Zoology* **61,** 2556–2573.

Otake, T., Hirokawa, J., Fujimoto, H. & Imaizumi, K. (1995). Fine structure and function of the gut epithelium of pike eel larvae. *Journal of Fish Biology* **47,** 126–142.

Polo, A., Yúfera, M. & Pascual, E. (1992). Feeding and growth of gilthead seabream (*Sparus aurata* L.) larvae in relation to the size of the rotifer strain used as food. *Aquaculture* **103,** 45–54.

Pisam, M., Boeuf, G., Prunet, P. & Rambourg, A. (1990). Ultrastructural features of mitochondria-rich cells in stenohaline freshwater and seawater fishes. *American Journal of Anatomy* **187,** 21–31.

Rønnstad, I., Koven, W. M., Tandler, A., Harel, M. & Fyhn, H. J. (1994). Energy metabolism during development of eggs and larvae of gilthead sea bream (*Sparus aurata*). *Marine Biology* **120,** 187–196.

Sarasquete, M. C., Polo, A. & González de Canales, M. L. (1993). A histochemical and immunohistochemical study of digestive enzymes and hormones during the larval development of the sea bream, *Sparus aurata* L. *Histochemical Journal* **25,** 430–437.

Sarasquete, M. C., Polo, A. & Yúfera, M. (1995). Histology and histochemistry of the development of the digestive system of larval gilthead seabream, *Sparus aurata* L. *Aquaculture* **130,** 79–92.

Segner, H., Burkhardt, P., Avila, E. M., Juario, J. V. & Storch, V. (1987*a*). Nutrition-related histopathology of the intestine of milkfish *Chanos chanos* fry. *Diseases of Aquatic Organisms* **2,** 99–107.

Segner, H., Burkhardt, P., Avila, E. M., Storch, V. & Juario, J. V. (1987*b*). Effects of chlorella-feeding on larval milkfish, *Chanos chanos*, as evidenced by histological monitoring. *Aquaculture* **67,** 113–116.

Segner, H., Rösch, R., Verreth, J. & Witt, U. (1993). Larval nutritional physiology: studies with *Clarias gariepinus, Coregonus lavaretus* and *Scophthalmus maximus*. *Journal of the World Aquaculture Society* **24,** 121–134.

Seligman, A. M., Wasserkrug, H. L. & Hanker, J. S. (1966). A new staining method (OTO) for enhancing contrast of lipid-containing membranes and droplets in osmium tetroxide-fixed tissue with osmiphilic thiocarbohydrazide (TCH). *Journal of Cell Biology* **30,** 424–432.

Sire, M. F. & Vernier, J. M. (1980). Lipid staining on semithin sections with Sudan Black B or Nile Blue sulphate. Application to intestinal fat absorption. *Acta Histochemica et Cytochemica* **13,** 193–201.

Sire, M. F. & Vernier, J. M. (1981). Étude ultrastructurale de la synthèse de chylomicrons au cours de l'absorption intestinale des lipides chez la Truite. Influence de la nature des acides gras ingérés. *Biology of the Cell* **40,** 47–62.

Smith, S. A., Caceci, T., Marei, H. E-S. & El-Habback, H. A. (1995). Observations on rodlet cells found in the vascular system and extravascular space of angelfish (*Pterophyllum scalare scalare*). *Journal of Fish Biology* **46,** 241–254.

Spurr, A. R. (1969). A low-viscosity epoxy resin embedding medium for electron microscopy. *Journal of Ultrastructure Research* **26,** 31–43.

Stroband, H. W. J. & Debets, F. M. H. (1978). The ultrastructure and renewal of the intestinal epithelium of the juvenile grasscarp, *Ctenopharyngodon idella* (Val.). *Cell and Tissue Research* **187,** 181–200.

Stroband, H. W. J. & Dabrowski, K. R. (1979). Morphological and physiological aspects of the digestive system and feeding in freshwater fish larvae. In *La Nutrition des Poissons* (Fontaine, M., ed.), pp. 355–376. Paris: CNERNA.

Tytler, P. & Ireland, J. (1994). Drinking and water absorption by the larvae of herring (*Clupea harengus*) and turbot (*Scophthalmus maximus*). *Journal of Fish Biology* **44,** 103–116.

Vernier, J. M. & Sire, M. F. (1986). Is the Golgi apparatus the obligatory final step for lipoprotein secretion by intestinal cells? *Tissue and Cell* **18,** 447–460.

Watanabe, Y. (1981). Ingestion of horseradish peroxidase by intestinal cells in larvae or juveniles of some teleosts. *Bulletin of the Japanese Society of Scientific Fisheries* **47,** 1299–1307.

Watanabe, Y. (1982). Intracellular digestion of horseradish peroxidase by the intestinal cells of teleost larvae and juveniles. *Bulletin of the Japanese Society of Scientific Fisheries* **48,** 37–42.

Watanabe, Y. (1984*a*). An ultrastructural study of intracellular digestion of horseradish peroxidase by the rectal epithelium cells in larvae of a freshwater cottid fish *Cottus nozawae*. *Bulletin of the Japanese Society of Scientific Fisheries* **50,** 409–416.

Watanabe, Y. (1984*b*). Morphological and functional changes in rectal epithelium cells of pond smelt during postembryonic development. *Bulletin of the Japanese Society of Scientific Fisheries* **50,** 805–814.

Watanabe, Y. & Sawada, N. (1985). Larval development of digestive organs and intestinal absorptive functions in the freshwater goby *Chaenogobius annularis*. *Bulletin of Tohoku Regional Fisheries Research Laboratory* **47,** 1–10.

Yúfera, M., Polo, A. & Pascual, E. (1993*a*). Changes in chemical composition and biomass during the transition from endogeneous to exogeneous feeding of *Sparus aurata* L. (Pisces, Sparidae) larvae reared in the laboratory. *Journal of Experimental Marine Biology and Ecology* **167,** 149–161.

Yúfera, M., Pascual, E., Polo, A. & Sarasquete, M. C. (1993*b*). Effect of starvation on the feeding ability of gilthead seabream (*Sparus aurata* L.) larvae at first feeding. *Journal of Experimental Marine Biology and Ecology* **169,** 259–272.

Yúfera, M., Sarasquete, M. C. & Fernández-Díaz, C. (1996). Testing protein-walled microcapsules for the rearing of first-feeding gilthead sea bream (*Sparus aurata* L.) larvae. *Marine and Freshwater Research* **47,** 211–216.